HHS Public Access

Author manuscript

Sci Immunol. Author manuscript; available in PMC 2017 May 18.

Published in final edited form as:

Sci Immunol. 2017 January ; 2(7): . doi:10.1126/sciimmunol.aaj2195.

Complement C5a Receptor is the Key Initiator of Neutrophil Adhesion Igniting Immune Complex-induced Arthritis

Yoshishige Miyabe[1], **Chie Miyabe**[1], **Thomas T. Murooka**[1], **Edward Y. Kim**[1], **Gail A. Newton**[3], **Nancy D. Kim**[1], **Bodduluri Haribabu**[2], **Francis W. Luscinskas**[3], **Thorsten R. Mempel**[1], and **Andrew D. Luster**[1,*]

[1]Center for Immunology and Inflammatory Diseases, Division of Rheumatology, Allergy and Immunology, Massachusetts General Hospital, Harvard Medical School, Boston, Massachusetts, USA

[2]James Graham Brown Cancer Center, University of Louisville, Louisville, Kentucky, USA

[3]Vascular Research Division, Brigham and Women's Hospital, Harvard Medical School, Boston, Massachusetts, USA

Abstract

The deposition of immune complexes (IC) in tissues induces a "type III hypersensitivity" that results in tissue damage and underlies the pathogenesis of many autoimmune diseases. The neutrophil is the first immune cell recruited into sites of IC deposition and plays a critical role in shaping the overall tissue response. However, the mechanism by which IC *initiate* and *propagate* neutrophil infiltration into tissue is not known. Here, using intravital multiphoton joint imaging of IC-induced arthritis in live mice, we found that the complement C5a receptor (C5aR) was the key initiator of neutrophil adhesion on joint endothelium. C5a presented on joint endothelium induced β2 integrin-dependent neutrophil arrest, facilitating neutrophil spreading and transition to crawling, and subsequent leukotriene B_4 receptor (BLT1)-mediated extravasation of the first neutrophils. The chemokine receptor CCR1 promoted neutrophil crawling on the joint endothelium while CXCR2 amplified late neutrophil recruitment and survival once in the joint. Thus, imaging arthritis has defined a new paradigm for type III hypersensitivity where C5a directly initiates neutrophil adhesion on the joint endothelium igniting inflammation.

INTRODUCTION

Deposition of antibody-antigen immune complexes (ICs) in tissues underlies the pathogenesis of a wide variety of autoimmune diseases, including systemic lupus

[*]*Correspondence:* Andrew D. Luster, MD, PhD, Massachusetts General Hospital-East, CNY 149-8 149 13th Street Charlestown, MA 02129, Tel: +1-617-726-5710, aluster@mgh.harvard.edu.

Author contributions: Y.M. designed and performed most experiments, analyzed and interpreted data and contributed to writing the manuscript; C.M. performed and analyzed flow cytometry, ELISA and IHC experiments; T.T.M, E.Y.K and T.R.M provided technical assistance for the MP-IVM experiments; G.A.N and F.W.L provided technical assistance for *in vitro* and *in vivo* adhesion assay; B.H. provided BLT1 antibody; N.D.K. provided K/BxN serum and technical assistance in working with the K/BxN serum transfer model of arthritis; A.D.L provided overall project supervision, contributed to the design of the experiments and wrote the manuscript.

Competing interests: The authors declare no competing financial interests.

erythematosus (SLE), rheumatoid arthritis (RA), vasculitis, serum sickness, post-streptococcal glomerulonephritis and cryoglobulinemia. In these diseases, collectively referred to as “type III hypersensitivity”, IC-deposition leads to a local inflammatory response characterized by immune cell infiltration and activation. The neutrophil is the first immune cell recruited into tissue, however, the mechanism by which deposited ICs *initiate* and *propagate* neutrophil infiltration into tissue is not known and is of considerable therapeutic importance (1).

The prevailing paradigm of “type III hypersensitivity” is that tissue-resident cells sense ICs through FcγRs and complement receptors and elaborate secondary mediators, such as TNF and IL-1, which activate endothelial cells (ECs) (1). Adhesion molecules and chemokines upregulated on the surface of activated ECs are then thought to promote neutrophil recruitment. While complement and FcγR activation have been variably implicated in the pathogenesis of IC-induced inflammation, their role in directly regulating neutrophil recruitment has not been elucidated.

The pathogenesis of IC-mediated disease has been interrogated in a variety of mouse models, including models of IC-induced inflammation of the skin, cremaster muscle, kidney, peritoneum, lung and joint (2–14). In the reverse passive cutaneous Arthus reaction, the inflammatory response in the skin is dependent on mast cell FcγR activation but independent of complement activation (2–4). In contrast, neutrophil FcγR activation is required for inflammation in models of IC-induced cremaster muscle and joint inflammation (5, 6), while tissue-resident macrophage FcγR activation is required in kidney, peritoneal and lung IC models (7–10). Inflammation in the cremaster muscle and kidney IC model are similar to the skin model in that they are independent of complement C3 and C5a (5, 8) while the peritoneal model is partially dependent on C5a (11, 12). C5a indirectly contributes to IC-mediated lung and peritoneal inflammation by activated FcγRs on resident macrophages (9, 10). In the K/BxN model of IC-induced arthritis, C5a is required for the development of arthritis (6, 14), although the mechanism by which it contributes to neutrophil recruitment and joint inflammation is not clear. Thus, there are important differences in the critical inducers of IC-induced inflammation depending on the organ where they are deposited, however, the mechanisms underlying these differences have not been elucidated to date.

In the K/BxN model, IgG autoantibodies to the ubiquitous glycolytic enzyme glucose-6-phosphate isomerase (GPI) form ICs with GPI and are preferentially deposited on the cartilage surface of the joint where they led to the local activation of the alternative complement pathway (AP) (14, 15). This model has similarities to human RA where joint tissue is frequently covered with ICs, and autoantibodies to ubiquitously expressed citrullinated self protein antigens (ACPAs) are present in the majority of patients with RA (16). As in other IgG IC-mediated diseases, neutrophil infiltration into the joint is critical for arthritis in the K/BxN mouse model as it is for joint inflammation in RA (17). Once in the joint, neutrophils become activated and release powerful proteases, cytokines, chemokines, and neutrophil extracellular traps (NETs) (18). Thus, neutrophils are essential initiators of IC-induced inflammation, including in the K/BxN model of arthritis as well as in RA. Neutrophils not only induce tissue destruction themselves, but also profoundly influence the

biology of other immune and structural cells of tissue, including in the joint that lead to RA (18). Therefore, understanding the molecular mechanisms controlling the entry of neutrophils into tissues, such as the joint, could be broadly helpful in understanding the pathogenesis of IC-induced inflammation and aid in the development of new therapies.

The β2 integrin LFA-1 and four neutrophil chemoattractant receptors (CARs), C5aR the leukotriene B4 receptor 1 (BLT1), the CC chemokine receptor 1 (CCR1), and the CXC chemokine receptor 2 (CXCR2), are all required on neutrophils for the development of arthritis in the K/BxN model of autoantibody IC-induced arthritis (6, 14, 19–22). While we have been able to suggest a temporal order for the requirement of these diverse CARs (23), we have not been able to decipher their respective functional roles in controlling neutrophil entry into the joint using traditional endpoint analysis. Further, it is not known what induces the very first neutrophils to enter the joint to initiate arthritis in this model. In fact, it has been proposed that sentinel tissue dwelling neutrophils are the key cell that initiates inflammation in this model of IC-induced tissue inflammation (24).

Recent advances in imaging technology have provided unprecedented views into immune cell migration in live animals that have deepened our understanding of the molecular control of immune cell trafficking into tissue *in vivo* (25). This process begins with the capture of free-flowing leukocytes on the vessel wall, followed by 1) *tethering and rolling* on the vessel wall in the direction of flow, 2) *firm arrest* on the endothelium, 3) release from arrest, *spreading out and crawling* in all directions on the vessel to locate a receptive location for 4) *transendothelial migration* (TEM) to extravasate into the tissue (26). Thus, applying MP-IVM to study IC-induced inflammation in the joint has the potential to take our understanding of IC-induced inflammation and immune cell entry into the joint to an entirely new level by allowing the real time visualization of the events that lead to arthritis in live mice.

Here, using a new joint imaging technique in live mice, we demonstrate that C5a is specifically presented on joint endothelium where it directly initiates neutrophil adhesion through its receptor C5aR expressed on neutrophils, igniting joint inflammation in a model of IC-induced arthritis.

RESULTS

C5aR is required for neutrophil adhesion in immune complex-induced arthritis

Multiple chemoattractant receptors (CARs) expressed on neutrophils are required for the development of joint inflammation in the K/BxN serum transfer model of arthritis (Fig. 1A). C5aR and BLT1 are absolutely required for arthritis as is the enzyme 5-lipoxgenase (5-LO) (*Alox5*$^{-/-}$), which is required for the generation of LTB_4, the BLT1 ligand. The chemokine receptors CCR1 and CXCR2 also contribute importantly to the development of arthritis and together are absolutely required for arthritis (Fig. 1A). These endpoint studies while informative are not able to ascertain the individual respective roles of the CA pathways in the control of neutrophil entry into the joint.

We have adapted MP-IVM in live mice to image the individual roles of the CARs implicated in neutrophil recruitment into the joint and the development of arthritis in real time (27). We have used *LysM*-GFP mice where expression of the green fluorescent protein (GFP) is driven by the lysozyme M promoter, resulting in GFP positive neutrophils and monocytes, to visualize neutrophil migratory behavior in the joints *in vivo*. Imaging joints of control (no arthritis) and arthritic wild type (WT)-*LysM*-GFP mice revealed the applicability of this technique (Fig. 1B, C; movie S1). Control mice had very few neutrophils visibly interacting with blood vessels of the joint and no neutrophils were visible outside of blood vessels (Fig. 1B; movie S1). In contrast, on day 7 following arthritogenic serum transfer (AST), neutrophils were detected adhered to blood vessels. This included cells that were still round and firmly arrested as well as cells that had spread out and were crawling on the endothelium in multiple directions (Fig. 1C; movie S1). In addition, many neutrophils were also seen outside of blood vessels, and were observed to be actively mobile and moving in multiple directions in inflamed joints (Fig. 1C; movie S1).

To reveal how deficiency in CARs might influence neutrophil migratory behavior in the joint, we imaged *Blt1*-KO-, *C5ar*-KO-, *Alox-5*-KO-, *Ccr1*-KO-, *Cxcr2*-KO- and *Ccr1-Cxcr2*-DKO-*LysM*-GFP mice 7 days after AST. We observed a striking phenotype in *C5ar*-KO mice: Neutrophils were not able to adhere to blood vessels of the joint (Fig. 1D; movie S1). The number of newly adherent neutrophils in *C5ar*-KO-*LysM*-GFP mice was dramatically less than other CARs-KO mice during the 30 mins of observation (Fig. 1J). In contrast, neutrophils were able to adhere to joint blood vessels in the other CAR-KO and *Alox-5*-KO mice on day 7 after AST (Fig. 1E–I; movie S1). However, the number of newly extravasated neutrophils that entered the tissue during the 30 mins of observation was markedly less in all CARs-KO and *Alox-5*-KO mice compared WT mice (Fig. 1K). These data demonstrate that C5aR plays a role in initiating neutrophil adhesion in the model, and that the other CARs participate in the process of neutrophil entry into the joint but at later stages in the process.

Cell intrinsic role for C5aR in neutrophil adhesion in the inflamed joint

To study the cell intrinsic role for each CAR in neutrophil migratory behavior in the setting of full-blown arthritis, we imaged joints 2 hours after adoptively transferring purified *Actin*-RFP-WT and *Actin*-GFP-CAR-KO neutrophils into WT mice that had received AST 7 days prior (fig. S1A). We confirmed that *Actin*-RFP-WT and *Actin*-GFP-CAR-KO neutrophils were present in a 1:1 ratio in the blood (fig. S1B). In these experiments, we were able to analyze neutrophil recruitment according to three defined sequential phases of the leukocyte migration cascade: firm arrest, spreading/crawling and extravasation (Fig. 2A). As was observed in *C5ar*-KO mice, markedly fewer *C5ar*-KO neutrophils were observed arrested and crawling on joint blood vessels compared to WT neutrophils when co-transferred into WT mice with arthritis (Fig. 2B, G, H). In contrast, other CAR-KO neutrophils did not display any defect in arrest or crawling compared with co-adoptively transferred WT neutrophils (Fig. 2C–H). However, as was observed for gene-deficient mice, adoptively transferred CAR-KO neutrophils studied had impaired extravasation when compared to co-adoptively transferred WT neutrophils (Fig. 2I). In addition, there was a marked delay in the time to firm arrest, spreading/crawling and extravasation for *C5ar*-KO neutrophils compared

to WT neutrophils while there was only a delay in the time to extravasation for the other CAR-KO neutrophils studied (fig. S1C). As might be expected in the setting of full-blown arthritis, the phenotype of adoptively transferred CAR-KO neutrophils was less dramatic than what was observed for neutrophils in CAR-KO mice where all neutrophils were CAR-deficient and mice had no evidence of joint inflammation.

To confirm the cell intrinsic role of C5aR in neutrophil adhesion and the cell intrinsic role of the other CARs in neutrophil extravasation, we generated mixed bone marrow chimeric (BMC) mice (fig. S2A). In these mice, BM cells from WT-*Actin*-RFP and CARs-KO-*Actin*-GFP mice were transferred in a 1:1 ratio into irradiated WT mice to determine the cell intrinsic effect of CAR-deficiency in mice over the entire course of arthritis development (fig. S2B). All of the mixed BMC mice developed arthritis following AST, although as might be expected, mixed BMC mice developed less severe arthritis than BMC control mice (WT BM into irradiated WT mice) (Fig. 3A). Again, markedly fewer *C5ar*-KO neutrophils were observed sticking to the joint endothelium, compared to WT neutrophils in these mixed BMC that developed arthritis (Fig. 3B, F). As was seen in the adoptive transfer experiments, the other CAR-KO neutrophils studied did not exhibit defects in adhesion to the joint endothelium, compared with WT neutrophils in arthritic BMC mice (Fig. 3C–F). However, all of the CAR-KO neutrophils studied in the mixed BMC mice had impaired extravasation compared to WT neutrophils following AST (Fig. 3G). Again, as might be expected, the phenotype of CAR-KO neutrophils in the mixed BMC arthritic mice was less dramatic than what was observed for neutrophils in CAR-KO mice where all neutrophils were CAR deficient and mice had no evidence of joint inflammation. These data confirm the conclusion that C5aR is uniquely required for initial neutrophil adhesion in this model, whereas other CARs contribute to extravasation into inflamed joints.

C5aR and CCR1 mediate neutrophil-endothelium interactions at different stages of the adhesion cascade

In the co-adoptive transfer experiments, we found that within 5 mins after arrest on the endothelium in arthritic joints, WT, *Ccr1*-, *Cxcr2*-, *Ccr1-Cxcr2*- and *Blt1*-KO neutrophils transformed their shape from round to amoeboid and initiated crawling (Fig. 4A; movie S2). In contrast, *C5ar*-KO neutrophils that managed to arrest on the endothelium in arthritic mice, maintained their round shape (circularity) as measured by Image J software, could not spread, and eventually detached (Fig. 4A, B; movie S2). Of note, ~40% of *C5ar*-KO arrested neutrophils detached in the adoptive transfer experiments, which is a phenomenon that was not observed for adoptively transferred WT neutrophils (Fig. 4C, D; movie S3). In addition, ~20% of adoptively transferred *Ccr1*-KO and *Ccr1-Cxcr2*-DKO neutrophils that initiated crawling were observed to detach from the endothelium, a phenomenon that was also not observed for WT adoptively transferred neutrophils that initiated crawling (Fig. 4E, F, G; movie S3). *Cxcr2*-KO crawling neutrophils did not detach, suggesting that detachment of *Ccr1-Cxcr2*-DKO crawling neutrophils was the result of a CCR1 deficiency.

We observed the same detachment phenotypes for *C5ar*-KO, *Ccr1*-KO and *Ccr1-Cxcr2*-DKO neutrophils in mixed BMC mice following serum transfer (fig. S2C–F). *C5ar*-KO neutrophils that were able to arrest were observed to detach from the endothelium of arthritic

joints in mixed *C5ar*-KO:WT BMC mice. Likewise, *Ccr1*-KO and *Ccr1-Cxcr2*-DKO neutrophils that initiated crawling were observed to detach from the endothelium of arthritis joints in *Ccr1*-KO:WT and *Ccr1-Cxcr2*-DKO:WT mixed BMC mice, respectively. These detachment phenotypes were not observed for WT neutrophils in these mice (fig. S2C–F). *Cxcr2*-KO neutrophils were not observed to detach after initiating crawling on joint endothelium in *Cxcr2*-KO:WT mixed BMC mice, again suggesting that detachment of *Ccr1-Cxcr2*-DKO crawling neutrophils was the result of a CCR1 deficiency. Taken together, these data suggest that C5aR signaling in neutrophils is also important for transition from firm arrest to spreading and crawling while CCR1 signaling is important to maintain cell crawling on the endothelium of the joint in this model as the cell probes for a receptive location to undergo TEM.

Early generation of C5a in the joint and retention on joint endothelium

To determine the kinetics of neutrophil CA generation in the model, we analyzed synovial fluid (SF) from control and arthritic mice on days 1, 3 and 7 after AST for levels of CAs by ELISA (Fig. 5A). In the joint space, C5a generation could be detected on day 1 after AST and rose to 76.33 ± 4.33 pM by day 3 and 856.7 ± 72.19 pM by day 7. LTB_4 production was detected beginning on day 3 and rose to 146.7 ± 27.28 pM by day 7. Chemokines were first detected on day 7. These data demonstrate that C5a is generated in the joint first followed by LTB_4 and then chemokines.

C5a deposition was detected on joint cartilage in mice with arthritis (day 7) but not in the joints of control mice (Fig. 5B, C). In addition, C5a immunoreactivity was also detected on VWF^+ endothelium of joints in arthritic mice, but not on the endothelium in the joints of control mice (Fig. 5D, E). Further, we did not detect C5a decorating VWF^+ endothelium of other organs from the same arthritic mice, including the aorta, coronary artery, superior vein cava, kidney and lung (fig. S3).

Since other basic CAs, like many of the chemokines, bind heparan sulfate proteoglycans (HSPG) on the surface of ECs, we tested if C5a also has this property. C5a bound directly to HSPG, and, as would be expected, heparin inhibited this interaction (Fig. 5F). In addition, C5a was able to bind to ECs and induce neutrophil adhesion *in vitro* (Fig. 5G). C5a binding to ECs was also inhibited by heparin, suggesting that C5a was binding to HSPG expressed on the surface of ECs. Thus, C5a generated in the joint space is captured by HSPG expressed on joint ECs and this initiates the neutrophil adhesion cascade in the joint.

C5a is a strong initiator of neutrophil adhesion in the joint

To directly demonstrate that C5a induces neutrophil adhesion *in vivo*, we developed an *in vivo* neutrophil adhesion and extravasation assay. Joints of control WT-*LysM*-GFP mice were surgically exposed and exogenous CAs were added to the surface of the exposed joint and imaged for 30 mins. All CAs tested were able to induce neutrophil adhesion and extravasation in the joint, compared to the PBS control (Fig. 6A–F; movie S4). Interestingly, C5a was the most efficacious CA at inducing adhesion and the least efficacious at inducing extravasation (Fig. 6G). In contrast, CXCL1 was the most efficacious at inducing neutrophil extravasation (Fig. 6H). C5a-induced neutrophil adhesion was dose-dependent (0.1–100.0

nM) with maximal adhesion seen at 10 nM (fig. S4A, B). Surprisingly, even though we imaged for 120 mins, C5a (10nM) did not induce neutrophil extravasation to nearly the same extent as CXCL1 (1nM) (fig. S4C, D). C5a-induced neutrophil adhesion was also observed in the joint of *Blt1*-KO and *Ccr1-Cxcr2*-DKO-*LysM*-GFP mice, suggesting that C5a-C5aR signaling *directly* induces adhesion (fig. S4E–G). These data suggest that C5a is a potent, direct initiator of neutrophil adhesion in the joint *in vivo*.

C5a induced neutrophil adhesion via β2 integrin activation

To determine if C5a-induced neutrophil adhesion was mediated by β2 integrins, we performed an *in vitro* adhesion on ICAM-1 coated plates. C5a induced neutrophil binding to ICAM-1, suggesting that C5a activates β2 integrins on neutrophils (Fig. 7A). Next, to detect which β2 integrin is important for C5a-mediated adhesion, we inhibited Mac-1 and LFA-1 using blocking antibodies. Inhibition of Mac-1 or LFA-1 partially inhibited C5a-induced neutrophil adhesion, and blocking both Mac-1 and LFA-1 was additive (Fig. 7A). These data suggest that C5a activates both LFA-1 and Mac-1 on neutrophils and induces neutrophil adhesion *in vitro*.

We then compared the expression levels of β2 integrin on BM, blood and SF neutrophils isolated from arthritic mice (day 7). LFA-1 and Mac-1 were highly expressed on the surface of neutrophils isolated form the BM, blood and SF of arthritic mice (fig. S5A). In addition, we confirmed that deficiency of CARs on neutrophils did not alter LFA-1 and Mac-1 levels on BM neutrophils (fig. S5B). Next, we analyzed if C5a-mediated neutrophil adhesion *in vivo* was mediated by β2 integrin activation using our *in vivo* adhesion assay. Blocking Mac-1 or LFA-1 inhibited C5a-induced neutrophil adhesion in the joint (Fig. 7B–E; movie S5). Dual blockade of LFA-1 and Mac-1 was even more effective than single blockade at inhibiting C5a-induced neutrophil adhesion *in vivo* (Fig. 7B, F; movie S5). Thus, these *in vivo* studies confirm our *in vitro* findings demonstrating that C5a-C5aR signaling on neutrophils activates β2 integrin, inducing neutrophil adhesion in the joint.

In addition, blockade of β2 integrins resulted in neutrophil detachment after C5a-induced adhesion (Fig. 6G–H; movie S6). LFA-1 blockade induced crawling neutrophils to detach from the endothelium (Fig. 6G; movie S6), while blockade of both Mac-1 and LFA-1 also induced arrested neutrophils to detach (Fig. 6H; movie S6). These data suggest that LFA-1 primarily mediates the strength of the interaction of C5aR-activated neutrophils with the endothelium.

CXCR2 ligands promote neutrophil recruitment and survival in the joint

The spontaneous production of neutrophil active chemokines from neutrophils isolated from the blood and joint of arthritic and control mice was determined by ELISA. Neutrophils isolated from the BM and blood of control mice did not spontaneous release neutrophil-active chemokines, including CXCL1, CXCL2 and CCL3. In contrast, neutrophils isolated from SF and blood, but not BM, of arthritic mice spontaneously produced CXCL2 (Fig. 8A), suggesting that activated neutrophils spontaneously release CXCL2.

We also analyzed the cell surface expression of the neutrophil active CARs studied here - C5aR, BLT1 CCR1 and CXCR2 - on neutrophils isolated from the BM, blood and SF of

arthritic mice. C5aR, BLT1 and CCR1 were expressed on BM, blood and SF neutrophils and the levels of these CARs were similar on neutrophils isolated from these three compartments (Fig 8B). In contrast, CXCR2 surface expression was low on BM neutrophils and increased markedly on neutrophils as they moved into the blood and then into the SF (Fig. 8B).

We also analyzed the kinetics of neutrophil accumulation in the SF of mixed BMC mice that had received AST 1, 3 and 7 days prior. In all mixed BMC mice, the ratio of WT and CAR-KO neutrophils in blood was equal over the entire course of arthritis (Fig. 8C–F). Initially, at day 1 after AST, the vast majority of neutrophils in the SF were WT (Fig. 8C–F). However the % *C5ar*-KO, *Blt1*-KO and *Ccr1*-KO neutrophils in SF increased over time (Fig. 8C, E and F). In contrast, *Cxcr2*-KO neutrophils did not increase in SF over time (Fig. 8D). These data suggest that CXCR2 promotes recruitment of *C5ar*-KO neutrophils into the arthritic joint after disease onset. In addition, we tested if CXCR2 also contributes to neutrophil survival once in the joint given reports that RA SF can prevent neutrophil apoptosis (28). SF neutrophils were isolated from the joints of arthritic mice (day 7 after AST) and incubated for 48 hours with CXCL1 and/or CXCL2. Apoptotic cells were identified as Annexin V^+ and necrotic cells as PI^+. Culture of SF neutrophils with CXCR2 ligands markedly reduced the population of Annexin V^+ neutrophils, suggesting apoptosis was dramatically inhibited compared to untreated SF neutrophils (Fig. 8H). These data suggest that in addition to amplifying neutrophil recruitment into the joint, CXCR2 also directly promotes the survival of neutrophils once in the inflamed joint.

DISCUSSION

While it is known that IC are important inducers of tissue inflammation, the mechanism by which IC deposition leads to the recruitment of immune cells into tissue is not known. Using a joint imaging technique in live mice and a murine model of IC-induced arthritis, we have identified a new role for C5a as the direct initiator of this process in the joint: C5a presented on joint endothelium activated C5aR on neutrophils inducing β2 integrin-dependent neutrophil adhesion. C5aR signaling also facilitated the transition of neutrophils from firm arrest to spreading and crawling for subsequent BLT1-dependent extravasation of the very first neutrophils into the joint. CCR1 contributed to the interaction of crawling neutrophils with the joint endothelium and CXCR2 amplified late neutrophil recruitment and promoted neutrophil survival once in the joint. Thus we have defined the roles of the CAR system in collaborating to control neutrophil recruitment into tissue in a type III hypersensitivity IC reaction. In so doing we have also demonstrated a role for C5a in directly initiating neutrophil recruitment and inflammation in the joint following IC deposition.

In the K/BxN model, circulating IC induce the production of vasoactive amines from radioresistant FcRγ-expressing cells that reside in the liver (13). This results in a localized transient vascular leak in the joint, which leads to the delivery of ICs into the joint space and their deposition on the surface of joint cartilage (13, 15). Given that the cartilage surface has a relative paucity of inhibitory complement regulatory proteins, such as decay accelerating factor, this leads to the local activation of the AP and the generation of C5a as ICs augment the spontaneous autoactivation of C3 in a process termed “tick-over” (15, 29). Consistent with this hypothesis, C3 is also required for arthritis in this model (14). C3 and its receptor

C3aR have also been implicated in RA pathogenesis (30), and AP activation has been associated with disease activity in adult and juvenile RA (31, 32).

Our data now demonstrate that C5a specifically decorates the inflamed joint endothelium and this is critical for activation of β2 integrins on neutrophils and the adhesion of the very first neutrophils, which initiates joint-specific inflammation. We found that C5a was generated in the joint space prior to the generation of the other CAs. C5aR was expressed on blood neutrophils as well as those recovered from the BM and SF, demonstrating that C5aR can respond to endothelially presented C5a to induce initial neutrophil adhesion on joint blood vessels. C5a was able to bind directly to joint endothelium as well as to HSPG *in vitro* and both of these interactions were inhibited by heparin. Further, C5a superfused on joints in live mice was the most potent CA at inducing neutrophil adhesion and was the least efficacious at inducing extravasation. We therefore postulate that much like chemokines, locally produced C5a is bound by HSPG on EC and this retains C5a locally, presenting it to rolling neutrophils. It is also possible that similar to what has been proposed for chemokines, C5a generated in the joint is transported to the surface of ECs by an atypical CAR-like receptor, such as C5L2. In fact, atypical chemokine receptor ACKR1 could transport inflammatory chemokines from the ablumin to the lumin of blood vessels (33). It has also been reported that C5aR is expressed at low levels on EC, and that C5aR signaling can induce the expression of ICAM-1 on HUVECs *in vitro* as well as disrupt vascular integrity (34, 35), both of which could contribute to joint inflammation. In the K/BxN model, however, C5aR on ECs does not play a major role as BMC experiments demonstrated that C5aR was only required on hematopoietic cells for the development of arthritis (36).

In addition to mediating initial adhesion, C5aR signaling also played a role in the transition to spreading and crawling. In co-adoptive transfer experiments and in mixed BMC experiments, we found that adherent *C5ar*-KO neutrophils were prone to detach from the endothelium. This phenotype is something that was not observed for WT neutrophils. Thus, the strength and/or duration of arrest likely contribute to the ability of neutrophils to transition from firm arrest to spreading and crawling. Both Mac-1 and LFA-1 contributes to the strength of zymosan-activated neutrophil adhesion to ECs with LFA-1 playing a more important role (37). The intraluminal crawling that follows arrest and spreading is essential for TEM (38). In TNF-activated and CXCL2-superfused cremaster muscle venules, neutrophil arrest and crawling were mediated by β2-integrins and their ligands ICAM-1 and ICAM-2. Arrest was mainly mediated by LFA-1, whereas luminal crawling was mainly mediated by Mac-1 (38, 39). Our data demonstrated that C5a induced both Mac-1- and LFA-1-mediated neutrophil adhesion *in vitro* and *in vivo* and that LFA-1 played a more important role in mediating the strength of the interaction with the endothelium. Thus, C5a-C5aR signaling activates Mac-1 and LFA-1 on neutrophils for adhesion and interaction with the endothelium.

How other CARs collaborate with C5aR to induce adherent neutrophils to enter into the inflamed joint in this model is largely unknown. However, like *C5ar*-KO mice, *Alox-5*-KO and *Blt1*-KO mice are completely resistant to the development of arthritis in the K/BxN AST model (19, 21). Our *in vivo* imaging experiments demonstrated that neutrophils were not able to extravasate into the joint in these mice following AST. In contrast to neutrophils

in the *C5ar*-KO mice, however, neutrophils in *Alox-5*-KO and *Blt1*-KO mice were able to arrest and transition to crawling following AST. Neutrophils were not able to undergo TEM, however, suggesting that LTB_4-BLT1 signaling initiates the first neutrophil entry into the joint. Given that C5aR signaling is required for LTB_4 production in the model (36), and that C5a is generated prior to LTB_4, our data suggest that C5a-C5aR signaling initiates neutrophil adhesion and the production of LTB_4, which results in the initial entry of neutrophils into the joint, triggering the initiation of arthritis.

Once neutrophils enter the joint and initiate arthritis, C5aR and BLT1 were not absolutely required for neutrophil recruitment into the joint. Although our neutrophil co-adoptive transfer and mixed BMC experiments revealed a cell intrinsic role for C5aR for adhesion and BLT1 for neutrophil TEM, there was only a 50% inhibition of these processes compared to their complete absence when the mouse was completely deficient in C5aR or BLT1. The reason for these differences likely reflect the fact that in the co-adoptive transfer experiments and mixed BMC experiments WT neutrophils are present and enter the joint where they become activated and produce cytokines, such as IL-1, and chemokines, such as CXCL2, within the joint (20). In addition, neutrophil produced IL-1 induces neutrophil active chemokine production from fibroblast like synoviocytes and ECs, which likely then partially relieves the absolute requirement for C5aR and BLT. Consistent with this, our data demonstrate that production of CXCR2 ligands and CCR1 ligands in the joint occur later than the generation of C5a and LTB_4, consistent with the hypothesis that C5a and LTB_4 are required for adhesion and TEM of the very first neutrophils for disease onset, whereas chemokines mainly contribute to the amplification and sustainment of neutrophil recruitment after disease onset.

In this regard, we also found roles for the chemokine receptors CCR1 and CXCR2 for neutrophil recruitment and the pathogenesis of joint inflammation. *Ccr1*-KO neutrophils specifically detached after initiating crawling, a behavior that was not seen for WT or for any of the other CAR-deficient neutrophils studied, suggesting that CCR1 contributes to the interaction of neutrophils with the endothelium of the joint. CCR1 ligands are well known to bind HSPG on ECs (40). Thus, CCR1 appears to support neutrophil extravasation by facilitating the ability of neutrophils to crawl on the endothelium of inflamed joints to locate receptive locations for TEM. We have also found that CXCR2 is involved with the sustained accumulation of neutrophil in the joint at later time points. Our mixed BMC mice demonstrated that *Cxcr2*-KO neutrophils were not found in the SF even at later points. This was in contrast to *Blt1-, C5ar-* and *Ccr1*-KO neutrophils that accumulated in the SF over time. This suggests that CXCR2 plays a role not only in neutrophil recruitment into the joint, but also in neutrophil survival once in the SF. Along these lines, we found that CXCR2 ligands prevented apoptosis SF neutrophils. It is interesting to note that neutrophils are the main cell type found in RA SF, which has been shown to prevent neutrophil apoptosis (28).

SF neutrophils from arthritic mice spontaneously secreted high levels of CXCL2 as well as produce IL-1, which can induce CXCR2 ligand generation from resident cells in the joints (20). A recent study also demonstrated that IC can induce CXCL2 production from neutrophils, and that CXCL2 released from neutrophils can induce CXCL1 production from macrophages (41), suggested that neutrophils are well equipped to self-regulate their own

recruitment. Using an *in vivo* recruitment assay, we found that CXCL1 was the most efficacious CA at inducing neutrophil extravasation into the joint. We also found that levels of CXCR2 were higher on neutrophils isolated from the SF compared to the blood and BM of arthritic mice. Our data therefore demonstrate that CXCR2 is an important mediator of late neutrophil recruitment and possibly survival in the joint space of arthritic mice.

Thus imaging immune-complex induced arthritis has defined a new mechanism for a type III hypersensitivity where C5a directly initiates neutrophil adhesion on the joint endothelium, resulting in neutrophil recruitment into the joint and the development of arthritis. These conclusions have some important limitations. First, the mechanism described here for the joint is likely different from other organs where tissue-resident cells have been shown to play an important role in initiating inflammation, and where C5a indirectly contributes to inflammation by activating resident immune cells (9, 10). The unique environment of the joint with a paucity of resident immune cells may be a determining factor for the critical proximal role of C5a and C5aR in initiating IC-induced arthritis. Further, the prominent role for C5a described here many not be applicable to other models of RA or to human RA where the role of IC in driving joint inflammation is likely more heterogeneous.

In summary, imaging arthritis has identified a mechanism whereby the C5a-C5aR pathway directly controls neutrophil adhesion on the endothelium and then facilitates their transition to crawling for subsequent BLT1-mediated entry into the joint to ignite inflammation. We have also found new roles of CCR1 in mediating neutrophil crawling on the endothelium and CXCR2 in mediating neutrophil survival in the joints space. Thus, we have defined how the CAR system collaborates to control neutrophil entry into the joint following IC deposition (fig. S6), and in so doing have established a new paradigm for type III hypersensitivity.

MATERIALS & METHODS

Study design

The aim of this study was to use in vivo joint imaging in live mice to determine the respective roles of C5aR, BLT1, CCR1 and CXCR2 in the recruitment of neutrophils into the joint in an IC-induced model of arthritis. Age (8–10 week old)- and sex (only male)-matched WT and CARs-KO mice bred and housed in the same faculty at Massachusetts General Hospital were used for this study. The sample size was determined to achieve a power of 90%, accepting type I error rate of 0.05. Analysis of movies as well as *in vitro* adhesion assays and flow cytometry was performed by an investigator blinded to the experimental groups. Randomization and blinding were not used for *in vivo* joint imaging.

Mice

K/BxN mice were obtained by crossing KRN with NOD/LtJ mice (Jackson Laboratory). *Ltb4r1*$^{-/-}$ (42), *C5ar*$^{-/-}$ (43), *Alox-5*$^{-/-}$ (44), *Cxcr2*$^{-/-}$ (45) and *Ccr1*$^{-/-}$ (46), *LysM*-GFP (47) mice were maintained in our laboratory. Wild-type C57BL/6 mice were purchased from the Charles River. C57BL/6-Tg(CAG-EGFP)131Osb/LeySopJ (*Actin*-GFP) and B6.Cg-Tg(CAG-DsRed*MST)1Nagy/J (*Actin*-RFP) were purchased from Jackson laboratory.

Ccr1$^{-/-}$*Cxcr2*$^{-/-}$ mice were generated by crossing *Ccr1*$^{-/-}$ and *Cxcr2*$^{-/-}$ mice, CARs-KO-*LysM*-GFP and *Actin*-GFP mice were generated by crossing CARs-KO mice and WT-*LysM*-GFP or WT-*Actin*-GFP mice, and genotypes were confirmed by Transnetyx, Inc. All experiments were performed according to protocols approved by the Massachusetts General Hospital Subcommittee on Research Animal Care.

Serum Transfer and Arthritis Scoring

Pooled serum from 8-week-old arthritic K/BxN mice was transferred into recipient mice (100 μl) intraperitoneally (i.p.) on days 0 and 2 as described (27). Clinical arthritis was scored as described (27).

Multiphoton Intravital Microscopy and Image Analysis

To perform MP-IVM, the ankle joint located 100 to 150 μm below the skin surface of anaesthetized mice was depilated, microsurgically exposed and fixed by tissue bond to glass slide on the microscope stage as described (27). Multiphoton excitation was obtained through DeepSee and MaiTai Ti:sapphire lasers (Newport/Spectra-Physics) tuned to 820 and 920 nm to excite all fluorescent probes used. Stacks of 11 square optical sections with 4 μm z-spacing were acquired on an Ultima IV multiphoton microscope (Prairie Technologies) every 15s with optical zoom of 2× to provide image volumes 40 μm in depth and 307 μm in width. Emitted fluorescence was detected through 460/50, 525/50, 595/50, 660/40 band-pass filters and non-descanned detectors to generate four-color images. Sequences of image stacks were transformed into volume- rendered, time-lapse movies with Imaris software (Bitplane). (1) Imaging of endogeneous neutrophils: Imaging joints of WT or CARs-KO-*LysM*-GFP mice on day 7 after AST was observed for 30 mins. The number of neutrophils that were observed to newly stick, including arrest and crawling, and newly extravasate, was quantitated. Neutrophils were distinguished by their size, shape, and migratory behavior. (2) Imaging adoptively transferred neutrophils: BM neutrophils were isolated by EasySep kit as described (27). Total 1×10^7 isolated BM neutrophils (5×10^6 BM WT *Actin*-RFP and 5×10^6 BM CAR-KO Actin-GFP neutrophils) were transferred into arthritic WT mice on day 7 following AST, which were matched for the same clinical arthritis score. Joints were imaged for 120 mins after BM neutrophil transfers. Population of circulating WT-GFP$^+$ and CARs-KO-RFP$^+$ neutrophils were confirmed by flow cytometry. Neutrophils were scored for the number that arrested, crawled and extravasated during the observation period. Arrest was defined as a round shape cell that remained in the same position for at least 30 second. Crawling was defined as an amoeboid shape cell that crawled along the inside of blood vessel. Extravasation was defined as a neutrophil that had entered into the tissue (27). (3) *In vivo* adhesion assay: CAs [0.1pmol: C5a (R&D), CXCL1, CXCL2, CCL3 (PeproTech) and LTB_4 (Tocris Bioscience)] dissolved with sterile PBS (100μl) was placed on the joints of WT-*LysM*-GFP mice, and imaged for 30 mins. Mac-1 and/or LFA-1 antibodies or isotype control antibody (100μg/mouse) were intravenously injected 4 hrs before imaging (22). The number of new sticking neutrophils as well as extravasated neutrophils was quantitated. All data was analyzed by Imaris software. Circularity was calculated using Image J software where 1.0 represented a complete circle.

Generation of mixed BMC mice

Mixed BMC mice were generated according to established protocols (36). Four wks after reconstitution mixed BMC mice were used for experiments. Reconstitution was confirmed by flow cytometry of blood neutrophil counts at 4 wks after irradiation. BMC mice were used if ≥ 95% of neutrophils were of donor origin and WT and CAR-KO neutrophils were present in equal numbers.

Flow cytometry

Neutrophils were isolated from BM, blood and SF according to established methods (27). Cells were blocked with 2.4G2 anti-FcγRIII/II (BD Biosciences) and stained with the following antibodies: APC-conjugated anti-murine Ly6G, FITC-conjucated anti-murine CXCR2, PE-conjucated anti-murine C5aR, FITC-conjucated anti-murine CD11a, PE-conjucated anti-murine CD11b (Biolegend), PE-conjugated anti-murine CCR1 (R&D), biotinylated anti-murine BLT1 (3D7, provided by Dr. Haribabu). Biotinylated mouse IgG1 (R&D) for BLT1, FITC-conjugated rat-IgG2a (Biolegend) for CXCR2 and CD11a, or PE-conjugated rat-IgG2a (Biolegend) for C5aR, CD11b and CCR1 were used as isotype control antibodies. After washing, BLT1 and its isotype control were incubated with PE-conjugated-streptavidin (eBioscience). Flow cytometry was performed with FACS LSRFortessa (BD Bioscience) and analyzed with Flow Jo software. Neutrophils were identified as Ly6G-positive cells in the granulocyte gate of forward and side scatter plots (fig. S7).

Quantitation of chemoattractants

SF was collected (27) and analyzed by enzyme-linked immunosorbent assay (ELISA) for levels of CXCL1, CXCL2, CCL3, C5a (R&D) and LTB_4 (Thermo). Immunomagnetically purified neutrophils from BM, blood, and SF were incubated at 2×10^6/ml in RPMI, 10% FCS, 10 mM HEPES, 100 U/ml penicillin, 100 μg/ml streptomycin at 37°C, 5% CO_2 for 21 hr. Cell-free cell culture supernatants were assayed for CXCL1, CXCL2 and CCL3 (R&D) by ELISA.

Immunofluorescence staining

Paraffin-embedded tissue sections (4μm–thick sections) from control and arthritic mice were prepared as described (27). Sections were then blocked with protein block (DakoCytomation) for 15 mins and stained with rabbit anti-C5a polyclonal antibody (8μg/ml; Bioss antibodies), anti-VWF polyclonal antibody (8μg/ml; LifeSpan Biosciences), or normal rabbit IgG (Bioss antibodies) as an isotype control for 60 mins at 25°C. Alexa Fluor 488 or 555–conjugated donkey anti-rabbit IgG (Abcam) were used as secondary antibodies and incubated for 1 hour at 25°C. The slides were examined using a fluorescence microscope (Carl Zeiss).

C5a binding to HSPG

HSPG (5μg/ml; Sigma-Aldrich) was coated on 96 well assay plates (Coring) overnight at 25°C. After washing 3 times with PBS with Tween 20 (PBST), 1%FCS/PBS was added to each well for 60-min at 25°C to block and then washed 3 times. C5a (1nM; R&D) with or without heparin (80μg/ml; Hospira) was loaded onto the well and incubated for 20-min at

25°C. After washing 3 times with PBST, C5a detection antibody (200ng/ml per well; R&D) was incubated for 2-hr at 25°C and washed 3 times with PBST. Streptavidin-HRP (R&D) was incubated for 20-min at 25°C and washed 3 times with PBST. Substrate solution (Invitrogen) was loaded onto plate for 20-min and 2N H_2SO_4 was used as a stop solution. Absorbance at OD 450nm was evaluated with a SpectraMax Plus 384 (Molecular Device).

In vitro neutrophil adhesion assay

(1) Murine aortic endothelial cells were incubated at a concentration of 2×10^4/well in Complete Mouse Endothelial Cell Medium with Endothelial Cell Medium Supplement Kit (Cell Biologics) at 37℃, 5% CO_2 overnight. The following day, after washing softly 3 times with sterile PBS, BM neutrophils isolated from naïve WT mice (1×10^5/well) were loaded onto plates with or without C5a (1nM) and/or heparin (80μg/ml) and incubated for 20 mins. After removing non-adherent neutrophils by washing 3 times, the number of adherent neutrophils was enumerated using microscopy. (2) ICAM-1 (2.5 μg/ml) was coated onto 96 well plates overnight at 4°C. The following day, the plate was washed by sterile PBS 3 times. BM neutrophils were isolated from naïve WT mice in RPMI, 10% FCS, 10 mM HEPES, 100 U/ml penicillin, 100 μg/ml streptomycin and incubated with LFA-1 and/or Mac-1 blocking antibodies or isotype control antibody (40 μg/ml) for 20 mins at room temperature. BM neutrophils (1×10^5/well) were loaded onto plates with or without C5a (1nM) for 20mins at 37℃. After removing non-adherent neutrophils by washing 3 times, the number of adherent neutrophils was counted using microscopy.

Analysis of apoptosis

Leukocytes were isolated from the SF of arthritic mice and neutrophils were purified using Easy-Sep as previously described (48). Neutrophils (1×10^5/well) were loaded into 96 well plates, and incubated with or without CXCL1 (1nM) and/or CXCL2 (1nM) for 48 hours. Neutrophils were analyzed for the presence of apoptosis using an Annexin V-FITC apoptosis detecting kit (Sigma-Aldrich) and flow cytometry with FACS LSRFortessa.

Statistics

Data are expressed as the mean ±SEM. All statistical analyses were performed in Prism 5 (GraphPad Software). Means between two groups were compared with unpaired two-tailed Student's *t* test. P values less than 0.05 were considered significant.

Supplementary Material

Refer to Web version on PubMed Central for supplementary material.

Acknowledgments

We thank D. Mathis and C. Benoist (Harvard Medical School) for providing KRN mice.

Funding: Supported by National Institutes of Health R01AI050892 (A.D.L) and R01AI097053 (T.R.M.) and Rheumatology Research Foundation (A.D.L), Mallinckrodt Pharmaceutical Research Fellowship Award in Rheumatology Research, Pfizer ASPIRE Rheumatology Award and Japan Rheumatism Foundation Research Grant (Y.M).

References

1. Mayadas TN, Tsokos GC, Tsuboi N. Mechanisms of immune complex-mediated neutrophil recruitment and tissue injury. Circulation. 2009; 120:2012–2024. [PubMed: 19917895]
2. Sylvestre D, Clynes R, Ma M, Warren H, Carroll MC, Ravetch JV. Immunoglobulin G-mediated inflammatory responses develop normally in complement-deficient mice. J Exp Med. 1996; 184:2385–2392. [PubMed: 8976192]
3. Sylvestre DL, Ravetch JV. A dominant role for mast cell Fc receptors in the Arthus reaction. Immunity. 1996; 5:387–390. [PubMed: 8885871]
4. Sylvestre DL, Ravetch JV. Fc receptors initiate the Arthus reaction: redefining the inflammatory cascade. Science. 1994; 265:1095–1098. [PubMed: 8066448]
5. Stokol T, O'Donnell P, Xiao L, Knight S, Stavrakis G, Botto M, von Andrian UH, Mayadas TN. C1q governs deposition of circulating immune complexes and leukocyte Fcgamma receptors mediate subsequent neutrophil recruitment. J Exp Med. 2004; 200:835–846. [PubMed: 15466618]
6. Monach PA, Nigrovic PA, Chen M, Hock H, Lee DM, Benoist C, Mathis D. Neutrophils in a mouse model of autoantibody-mediated arthritis: critical producers of Fc receptor gamma, the receptor for C5a, and lymphocyte function-associated antigen 1. Arthritis Rheum. 2010; 62:753–764. [PubMed: 20191628]
7. Heller T, Gessner JE, Schmidt RE, Klos A, Bautsch W, Kohl J. Cutting edge: Fc receptor type I for IgG on macrophages and complement mediate the inflammatory response in immune complex peritonitis. J Immunol. 1999; 162:5657–5661. [PubMed: 10229794]
8. Stamatiades EG, Tremblay ME, Bohm M, Crozet L, Bisht K, Kao D, Coelho C, Fan X, Yewdell WT, Davidson A, Heeger PS, Diebold S, Nimmerjahn F, Geissmann F. Immune Monitoring of Trans-endothelial Transport by Kidney-Resident Macrophages. Cell. 2016; 166:991–1003. [PubMed: 27477514]
9. Shushakova N, Skokowa J, Schulman J, Baumann U, Zwirner J, Schmidt RE, Gessner JE. C5a anaphylatoxin is a major regulator of activating versus inhibitory FcgammaRs in immune complex-induced lung disease. J Clin Invest. 2002; 110:1823–1830. [PubMed: 12488432]
10. Godau J, Heller T, Hawlisch H, Trappe M, Howells E, Best J, Zwirner J, Verbeek JS, Hogarth PM, Gerard C, Van Rooijen N, Klos A, Gessner JE, Kohl J. C5a initiates the inflammatory cascade in immune complex peritonitis. J Immunol. 2004; 173:3437–3445. [PubMed: 15322209]
11. Hopken UE, Lu B, Gerard NP, Gerard C. Impaired inflammatory responses in the reverse arthus reaction through genetic deletion of the C5a receptor. J Exp Med. 1997; 186:749–756. [PubMed: 9271590]
12. Ramos BF, Zhang Y, Jakschik BA. Neutrophil elicitation in the reverse passive Arthus reaction. Complement-dependent and -independent mast cell involvement. J Immunol. 1994; 152:1380–1384. [PubMed: 8301139]
13. Binstadt BA, Patel PR, Alencar H, Nigrovic PA, Lee DM, Mahmood U, Weissleder R, Mathis D, Benoist C. Particularities of the vasculature can promote the organ specificity of autoimmune attack. Nat Immunol. 2006; 7:284–292. [PubMed: 16444258]
14. Ji H, Ohmura K, Mahmood U, Lee DM, Hofhuis FM, Boackle SA, Takahashi K, Holers VM, Walport M, Gerard C, Ezekowitz A, Carroll MC, Brenner M, Weissleder R, Verbeek JS, Duchatelle V, Degott C, Benoist C, Mathis D. Arthritis critically dependent on innate immune system players. Immunity. 2002; 16:157–168. [PubMed: 11869678]
15. Matsumoto I, Maccioni M, Lee DM, Maurice M, Simmons B, Brenner M, Mathis D, Benoist C. How antibodies to a ubiquitous cytoplasmic enzyme may provoke joint-specific autoimmune disease. Nat Immunol. 2002; 3:360–365. [PubMed: 11896391]
16. Willemze A, Trouw LA, Toes RE, Huizinga TW. The influence of ACPA status and characteristics on the course of RA. Nat Rev Rheumatol. 2012; 8:144–152. [PubMed: 22293763]
17. Wipke BT, Allen PM. Essential role of neutrophils in the initiation and progression of a murine model of rheumatoid arthritis. J Immunol. 2001; 167:1601–1608. [PubMed: 11466382]
18. Wright HL, Moots RJ, Edwards SW. The multifactorial role of neutrophils in rheumatoid arthritis. Nat Rev Rheumatol. 2014; 10:593–601. [PubMed: 24914698]

19. Kim ND, Chou RC, Seung E, Tager AM, Luster AD. A unique requirement for the leukotriene B4 receptor BLT1 for neutrophil recruitment in inflammatory arthritis. J Exp Med. 2006; 203:829–835. [PubMed: 16567386]
20. Chou RC, Kim ND, Sadik CD, Seung E, Lan Y, Byrne MH, Haribabu B, Iwakura Y, Luster AD. Lipid-cytokine-chemokine cascade drives neutrophil recruitment in a murine model of inflammatory arthritis. Immunity. 2010; 33:266–278. [PubMed: 20727790]
21. Chen M, Lam BK, Kanaoka Y, Nigrovic PA, Audoly LP, Austen KF, Lee DM. Neutrophil-derived leukotriene B4 is required for inflammatory arthritis. J Exp Med. 2006; 203:837–842. [PubMed: 16567388]
22. Watts GM, Beurskens FJ, Martin-Padura I, Ballantyne CM, Klickstein LB, Brenner MB, Lee DM. Manifestations of inflammatory arthritis are critically dependent on LFA-1. J Immunol. 2005; 174:3668–3675. [PubMed: 15749905]
23. Sadik CD, Luster AD. Lipid-cytokine-chemokine cascades orchestrate leukocyte recruitment in inflammation. J Leukoc Biol. 2012; 91:207–215. [PubMed: 22058421]
24. McDonald B, Kubes P. Chemokines: sirens of neutrophil recruitment-but is it just one song? Immunity. 2010; 33:148–149. [PubMed: 20732637]
25. Murooka TT, Mempel TR. Multiphoton intravital microscopy to study lymphocyte motility in lymph nodes. Methods Mol Biol. 2012; 757:247–257. [PubMed: 21909917]
26. Mayadas TN, Cullere X, Lowell CA. The multifaceted functions of neutrophils. Annu Rev Pathol. 2014; 9:181–218. [PubMed: 24050624]
27. Miyabe Y, Kim ND, Miyabe C, Luster AD. Studying Chemokine Control of Neutrophil Migration In Vivo in a Murine Model of Inflammatory Arthritis. Methods Enzymol. 2016; 570:207–231. [PubMed: 26921948]
28. Ottonello L, Cutolo M, Frumento G, Arduino N, Bertolotto M, Mancini M, Sottofattori E, Dallegri F. Synovial fluid from patients with rheumatoid arthritis inhibits neutrophil apoptosis: role of adenosine and proinflammatory cytokines. Rheumatology (Oxford). 2002; 41:1249–1260. [PubMed: 12421997]
29. Holers VM. Complement and its receptors: new insights into human disease. Annu Rev Immunol. 2014; 32:433–459. [PubMed: 24499275]
30. Neumann E, Barnum SR, Tarner IH, Echols J, Fleck M, Judex M, Kullmann F, Mountz JD, Scholmerich J, Gay S, Muller-Ladner U. Local production of complement proteins in rheumatoid arthritis synovium. Arthritis Rheum. 2002; 46:934–945. [PubMed: 11953970]
31. Trouw LA, Haisma EM, Levarht EW, van der Woude D, Ioan-Facsinay A, Daha MR, Huizinga TW, Toes RE. Anti-cyclic citrullinated peptide antibodies from rheumatoid arthritis patients activate complement via both the classical and alternative pathways. Arthritis Rheum. 2009; 60:1923–1931. [PubMed: 19565507]
32. Aggarwal A, Bhardwaj A, Alam S, Misra R. Evidence for activation of the alternate complement pathway in patients with juvenile rheumatoid arthritis. Rheumatology (Oxford). 2000; 39:189–192. [PubMed: 10725071]
33. Pruenster M, Mudde L, Bombosi P, Dimitrova S, Zsak M, Middleton J, Richmond A, Graham GJ, Segerer S, Nibbs RJ, Rot A. The Duffy antigen receptor for chemokines transports chemokines and supports their promigratory activity. Nat Immunol. 2009; 10:101–108. [PubMed: 19060902]
34. Albrecht EA, Chinnaiyan AM, Varambally S, Kumar-Sinha C, Barrette TR, Sarma JV, Ward PA. C5a-induced gene expression in human umbilical vein endothelial cells. Am J Pathol. 2004; 164:849–859. [PubMed: 14982839]
35. Jacob A, Hack B, Chen P, Quigg RJ, Alexander JJ. C5a/CD88 signaling alters blood-brain barrier integrity in lupus through nuclear factor-kappaB. J Neurochem. 2011; 119:1041–1051. [PubMed: 21929539]
36. Sadik CD, Kim ND, Iwakura Y, Luster AD. Neutrophils orchestrate their own recruitment in murine arthritis through C5aR and FcγR signaling. Proc Natl Acad Sci U S A. 2012; 109:E3177–3185. [PubMed: 23112187]
37. Ding ZM, Babensee JE, Simon SI, Lu H, Perrard JL, Bullard DC, Dai XY, Bromley SK, Dustin ML, Entman ML, Smith CW, Ballantyne CM. Relative contribution of LFA-1 and Mac-1 to neutrophil adhesion and migration. J Immunol. 1999; 163:5029–5038. [PubMed: 10528208]

38. Sumagin R, Prizant H, Lomakina E, Waugh RE, Sarelius IH. LFA-1 and Mac-1 define characteristically different intralumenal crawling and emigration patterns for monocytes and neutrophils in situ. J Immunol. 2010; 185:7057–7066. [PubMed: 21037096]

39. Phillipson M, Heit B, Colarusso P, Liu L, Ballantyne CM, Kubes P. Intraluminal crawling of neutrophils to emigration sites: a molecularly distinct process from adhesion in the recruitment cascade. J Exp Med. 2006; 203:2569–2575. [PubMed: 17116736]

40. Tanaka Y, Fujii K, Hübscher S, Aso M, Takazawa A, Saito K, Ota T, Eto S. Heparan sulfate proteoglycan on endothelium efficiently induces integrin-mediated T cell adhesion by immobilizing chemokines in patients with rheumatoid synovitis. Arthritis Rheum. 1998; 41:1365–1377. [PubMed: 9704634]

41. Li JL, Lim CH, Tay FW, Goh CC, Devi S, Malleret B, Lee B, Bakocevic N, Chong SZ, Evrard M, Tanizaki H, Lim HY, Russell B, Renia L, Zolezzi F, Poidinger M, Angeli V, St John AL, Harris JE, Tey HL, Tan SM, Kabashima K, Weninger W, Larbi A, Ng LG. Neutrophils Self-Regulate Immune Complex-Mediated Cutaneous Inflammation through CXCL2. J Invest Dermatol. 2016; 136:416–424. [PubMed: 26802238]

42. Tager AM, Dufour JH, Goodarzi K, Bercury SD, von Andrian UH, Luster AD. BLTR mediates leukotriene B(4)-induced chemotaxis and adhesion and plays a dominant role in eosinophil accumulation in a murine model of peritonitis. J Exp Med. 2000; 192:439–446. [PubMed: 10934232]

43. Hopken UE, Lu B, Gerard NP, Gerard C. The C5a chemoattractant receptor mediates mucosal defence to infection. Nature. 1996; 383:86–89. [PubMed: 8779720]

44. Goulet JL, Snouwaert JN, Latour AM, Coffman TM, Koller BH. Altered inflammatory responses in leukotriene-deficient mice. Proc Natl Acad Sci U S A. 1994; 91:12852–12856. [PubMed: 7809134]

45. Cacalano G, Lee J, Kikly K, Ryan AM, Pitts-Meek S, Hultgren B, Wood WI, Moore MW. Neutrophil and B cell expansion in mice that lack the murine IL-8 receptor homolog. Science. 1994; 265:682–684. [PubMed: 8036519]

46. Gao JL, Wynn TA, Chang Y, Lee EJ, Broxmeyer HE, Cooper S, Tiffany HL, Westphal H, Kwon-Chung J, Murphy PM. Impaired host defense, hematopoiesis, granulomatous inflammation and type 1-type 2 cytokine balance in mice lacking CC chemokine receptor 1. J Exp Med. 1997; 185:1959–1968. [PubMed: 9166425]

47. Faust N, Varas F, Kelly LM, Heck S, Graf T. Insertion of enhanced green fluorescent protein into the lysozyme gene creates mice with green fluorescent granulocytes and macrophages. Blood. 2000; 96:719–726. [PubMed: 10887140]

48. Miyabe Y, Kim ND, Miyabe C, Luster AD. Studying Neutrophil Migration In Vivo Using Adoptive Cell Transfer. Methods Mol Biol. 2016; 1407:179–194. [PubMed: 27271903]

Author Manuscript

Author Manuscript

Author Manuscript

One Sentence Summary

C5aR directly initiates neutrophil adhesion required for immune-complex induced arthritis

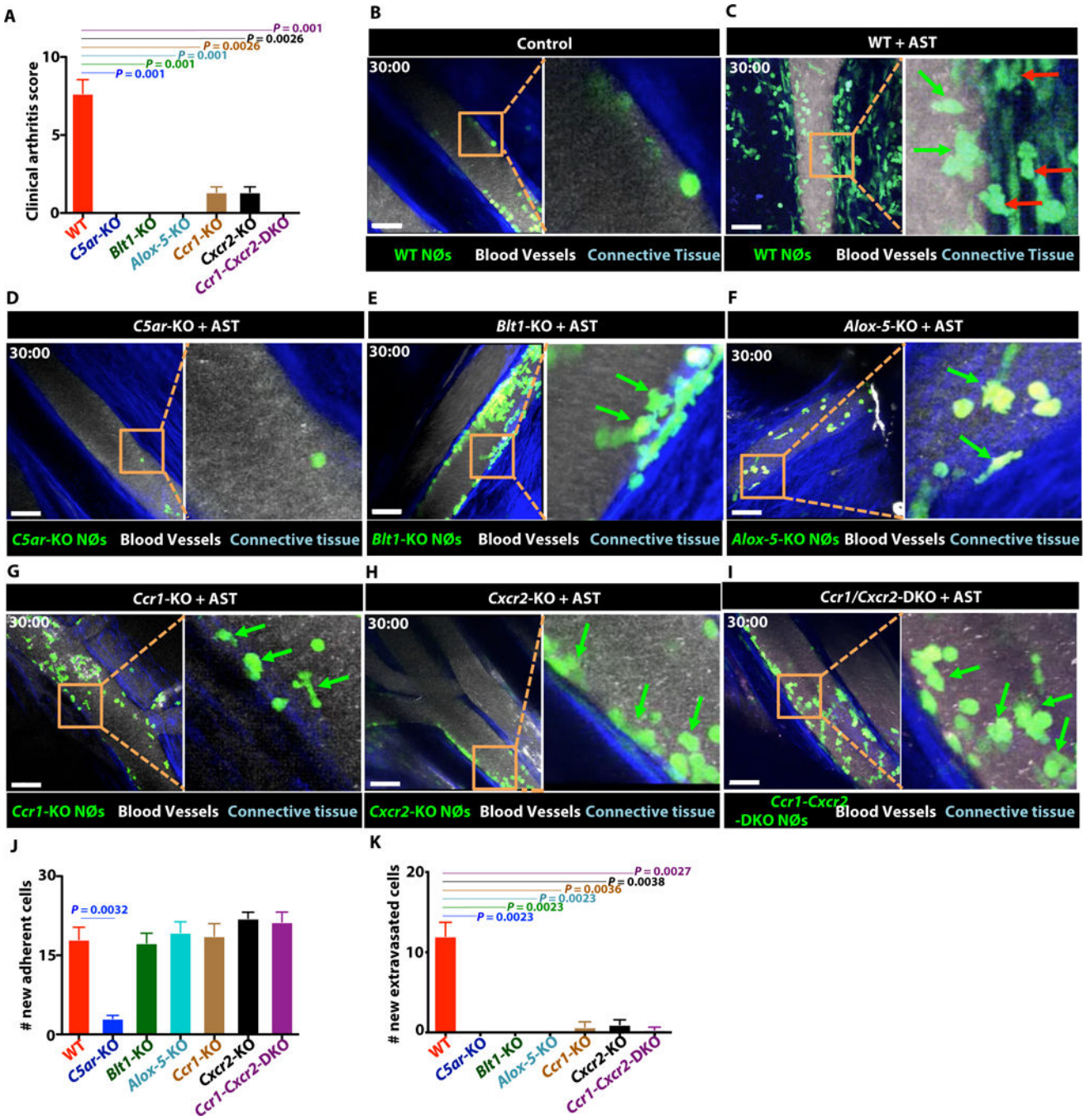

Figure 1. ***In vivo*** **imaging of inflammatory arthritis in live mice**

(**A**) Clinical arthritis score of WT and CAR-KO mice on day 7 after arthritogenic serum transfer (AST). (**B–I**) *In vivo* imaging of the joint in live mice. Data are representative of 3 independent experiments. (**B**) WT-*LysM*-GFP no AST. (**C–I**) WT or CAR-KO-*LysM*-GFP mice on day 7 following AST. (**C**) WT, (**D**) *C5ar*-KO, (**E**) *Blt1*-KO, (**F**) *Alox-5*-KO (**G**) *Ccr1*-KO (**H**) *Cxcr2*-KO and (**I**) *Ccr1-Cxcr2*-DKO mice. GFP: neutrophils; Blue: Connective tissue; Qdots: Blood vessels. Time in mins:secs. Scale bars represent 50 μm. (**J**) Number of newly adherent cells, and (**K**) newly extravasated cells in the joints during 30-

min recording. Data indicate mean ± SEM. n = 3 mice/group and P valve calculated using unpaired two-tails Student’s t-test

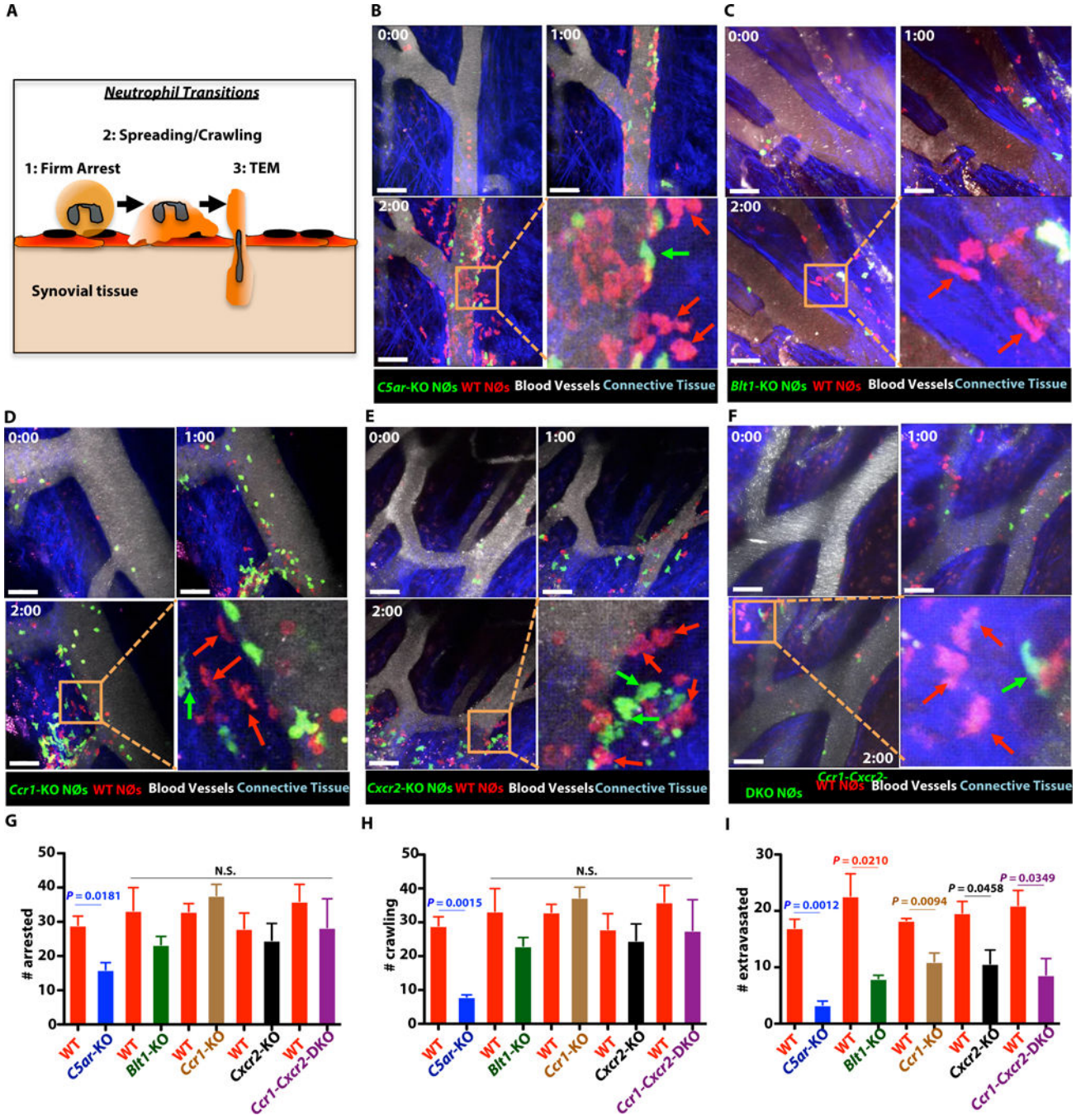

Figure 2. ***In vivo*** **imaging WT and CAR-KO neutrophils co-adoptively transferred into arthritic WT mice**

(**A**) Schematic of neutrophil migration cascade. (**B–F**) *In vivo* imaging of the joint after co-adoptive transfer of WT-*Actin*-RFP and CAR-KO-*Actin*-GFP purified neutrophils into WT mice that received AST 7 days prior. Data are representative of 3 independent experiments. (**B**) WT and *C5ar*-KO, (**C**) WT and *Blt1*-KO (**D**), WT and *Ccr1*-KO (**E**), WT and *Cxcr2*-KO and (**F**) WT and *Ccr1-Cxcr2*-DKO neutrophils. GFP: CAR-KO neutrophils; RFP: WT neutrophil; Blue: connective tissue; Qdots: Blood vessels. Scale bars represent 50 μm. Time

in hrs:mins. Green arrows shows extravasated CAR-KO neutrophils, and red arrows show extravasated WT neutrophils. (**G–I**) Quantitation of the number of new (**G**) arrested, (**H**) crawling, and (**I**) extravasated neutrophils; in the joint during the 120 min observed. Data indicate mean ± SEM. n = 3 mice/group, P value calculated using unpaired two-tails Student's t-test. N.S.- not statistically significant.

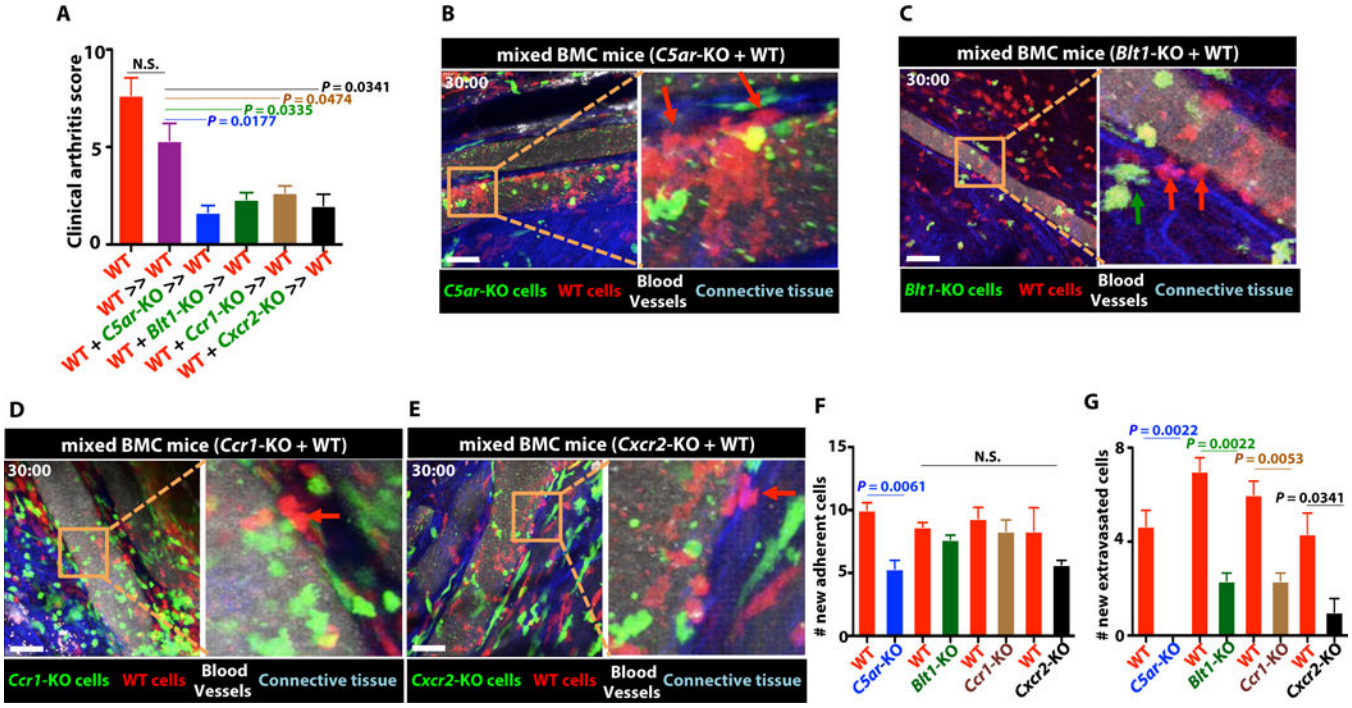

Figure 3. *In vivo* imaging joints of mixed bone marrow chimeric mice on day 7 after AST

(**A**) Clinical arthritis score on day 7 after AST. (**B–E**) Representative images the joint of mixed BMC mice on day 7 after AST. Mixed BMC mice were generated by the transfer of WT-*Actin*-RFP- and CAR-KO-*Actin*-GFP BM (1:1 ratio) into irradiated WT mice. While leukocytes other than neutrophils were fluorescently labeled in these experiments, neutrophils were easily identified by their size, shape and migratory properties. Data are representative of 3 independent experiments. (**B**) *C5ar*-KO-*Actin*-GFP and WT-*Actin*-RFP BM cells transferred into WT mice. (**C**) *Blt1*-KO-*Actin*-GFP and WT-*Actin*-RFP BM cells transferred into WT mice. (**D**) *Ccr1*-KO-*Actin*-GFP and WT-*Actin*-RFP BM cells transferred into WT mice. (**E**) *Cxcr2*-KO-*Actin*-GFP and WT-*Actin*-RFP BM cells transferred into WT mice. GFP: CARs-KO-cell, RFP: WT-cell, Blue: Connective tissue, Qdots: Blood vessels. Time in mins:secs. Scale bars represent 50 μm. (**F, G**) Quantitation of sticking cells and extravasated cells in the joint. (**A, F, G**) Data indicate mean ± SEM. n = 3 mice/group, P value calculated using unpaired two-tails Student's t-test. N.S.- not statistically significant.

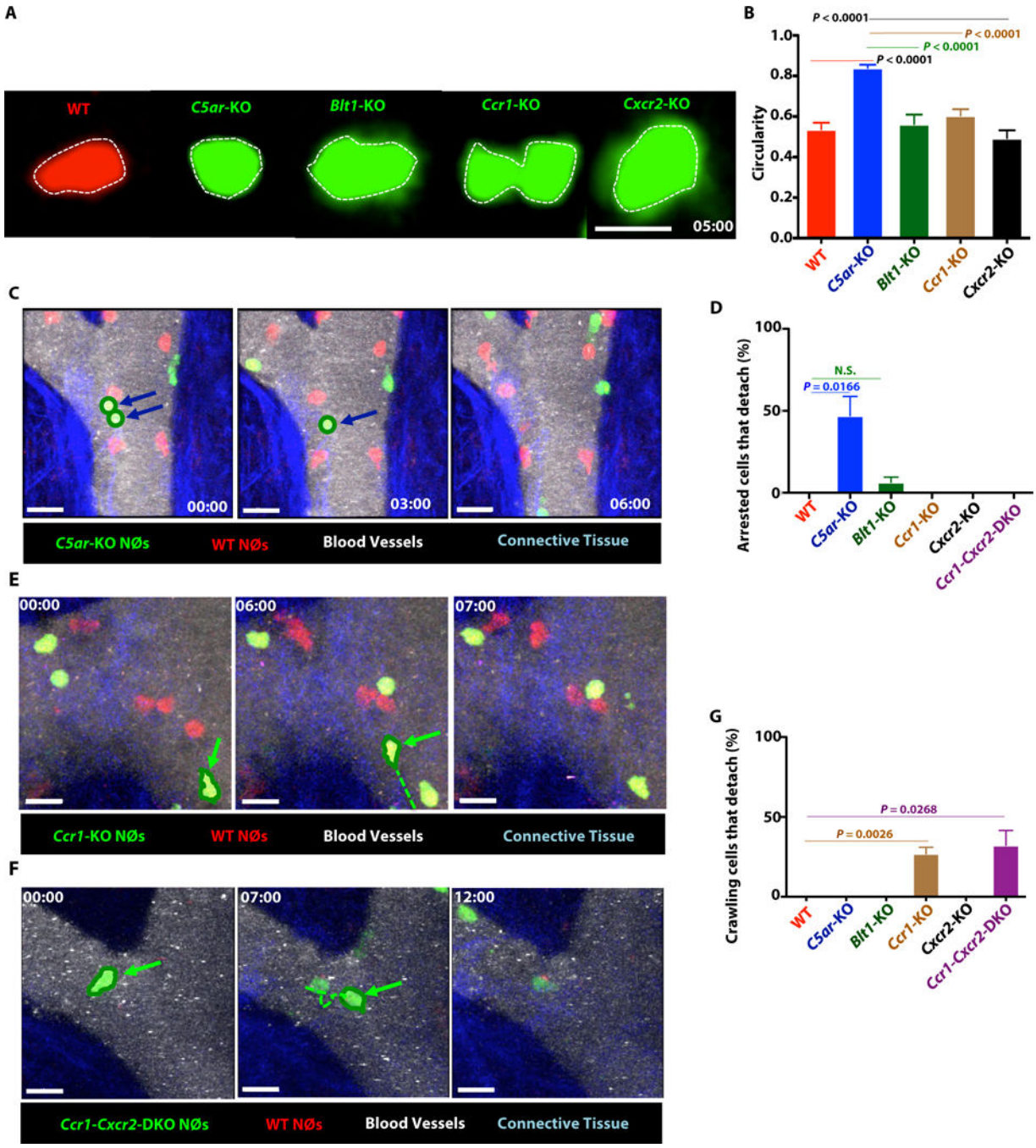

Figure 4. C5aR and CCR1 mediate interactions of neutrophils with the joint endothelium at different stages of the adhesion cascade

(**A**) Shape of WT and CAR-KO neutrophils 5 min after arrest. Broken white line outlines the shape of the neutrophils. Scale bars represent 10 μm. (**B**) Circularity of WT and CAR-KO neutrophils 5 mins after arrest. Data indicate mean ± SEM; n= 10 cells/genotype (**C–G**) *In vivo* joint imaging after adoptive transfer of WT-*Actin*-RFP and CAR-KO-*Actin*-GFP neutrophils into WT mice that received AST 7 days prior. Blue: Connective tissue; Qdots: Blood vessels. (**C**) WT and *C5ar*-KO neutrophils. Blue arrows indicate arrested cells that

detached. Time in mins:secs. Scale bars represent 10 μm. Data are representative of 3 independent experiments. (**D**) Quantitation of arrested cell that detached from the joint endothelium over 120 mins observation. (**E**) WT and *Ccr1*-KO and (**F**) WT and *Ccr1-Cxcr2*-DKO neutrophils. Green arrow indicates crawling cells that detach. Green broken line indicates the track of a mobile cell. Time in mins:secs. Scale bars represent 10 μm. (**G**) Quantitation of crawling cells that detach from the joint endothelium over 120 mins of observation (**C,E, F**) Data are representative of 3 independent experiments. (**D, G**) Data indicate mean ± SEM; n = 3 mice/group; P value calculated using unpaired two-tails Student's t-test. N.S.- not statistically significant.

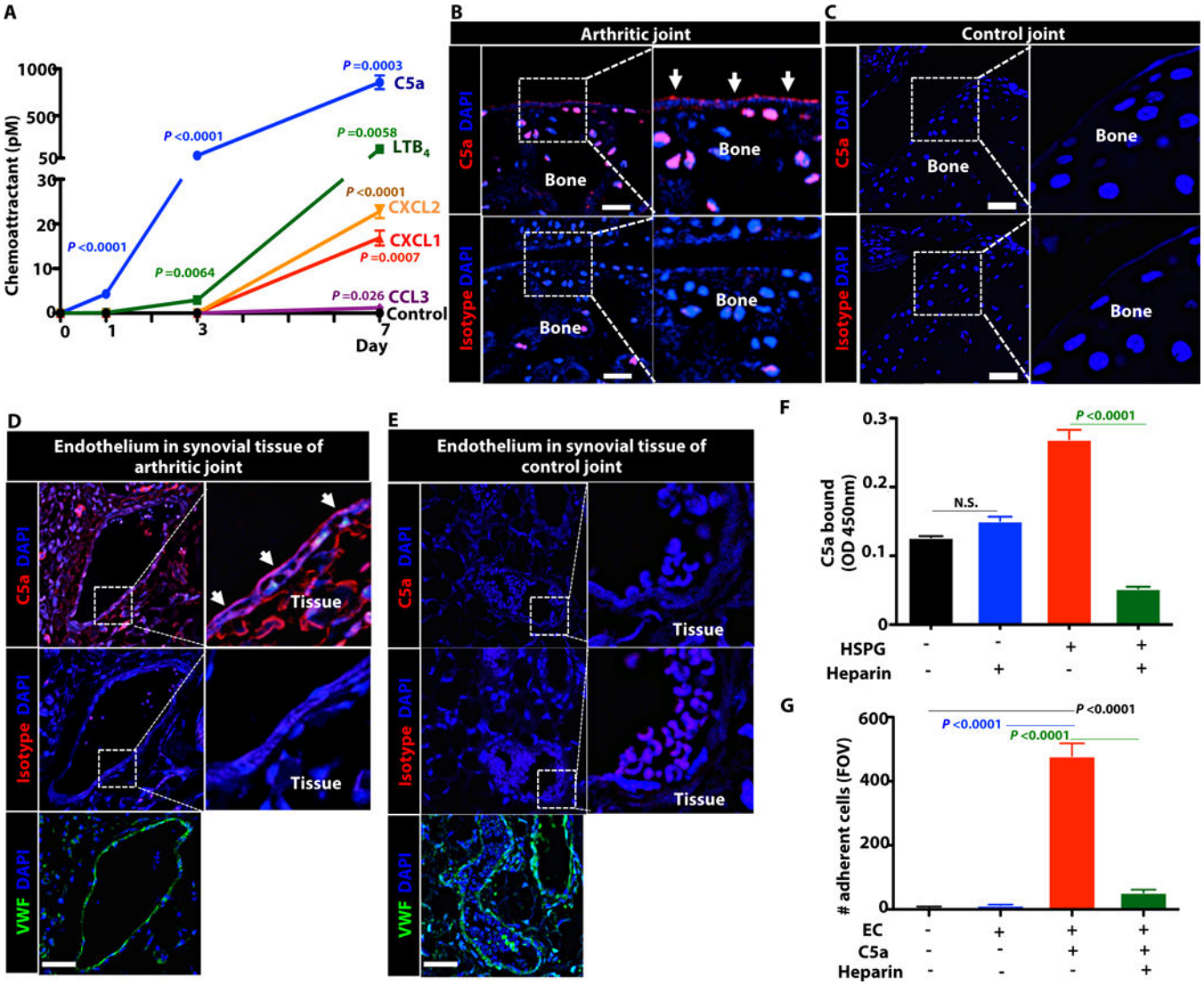

Figure 5. C5a expression and binding in the inflamed joint

(**A**) Levels of CAs in SF on days 0, 1, 3 and 7 following AST as determined by ELISA. n = 3 mice/time point (**B–E**) Immunofluorescence staining of joint tissue from arthritic mice on day 7 after AST (**B, D**) or control mice (**C, E**). Red: C5a; Green: VWF^{+}ECs; Blue: DAPI. Scale bars =50μm. Data are representative of 3 independent experiments. (**F**) *In vitro* binding assay. Amount of C5a bound to uncoated 96well assay plates or plates coated with HSPG (5μg/ml) in the presence or absence of heparin (80μg/ml) (**G**) *In vitro* adhesion assay. Number of BM neutrophils adherent to murine aortic endothelial cells that were pretreated with C5a (1nM) in the presence or absence of heparin (80μg/ml) (F,G) n = 3 independent experiments. Data indicate mean ± SEM; P value calculated using unpaired two-tails Student's t-test. N.S.- not statistically significant.

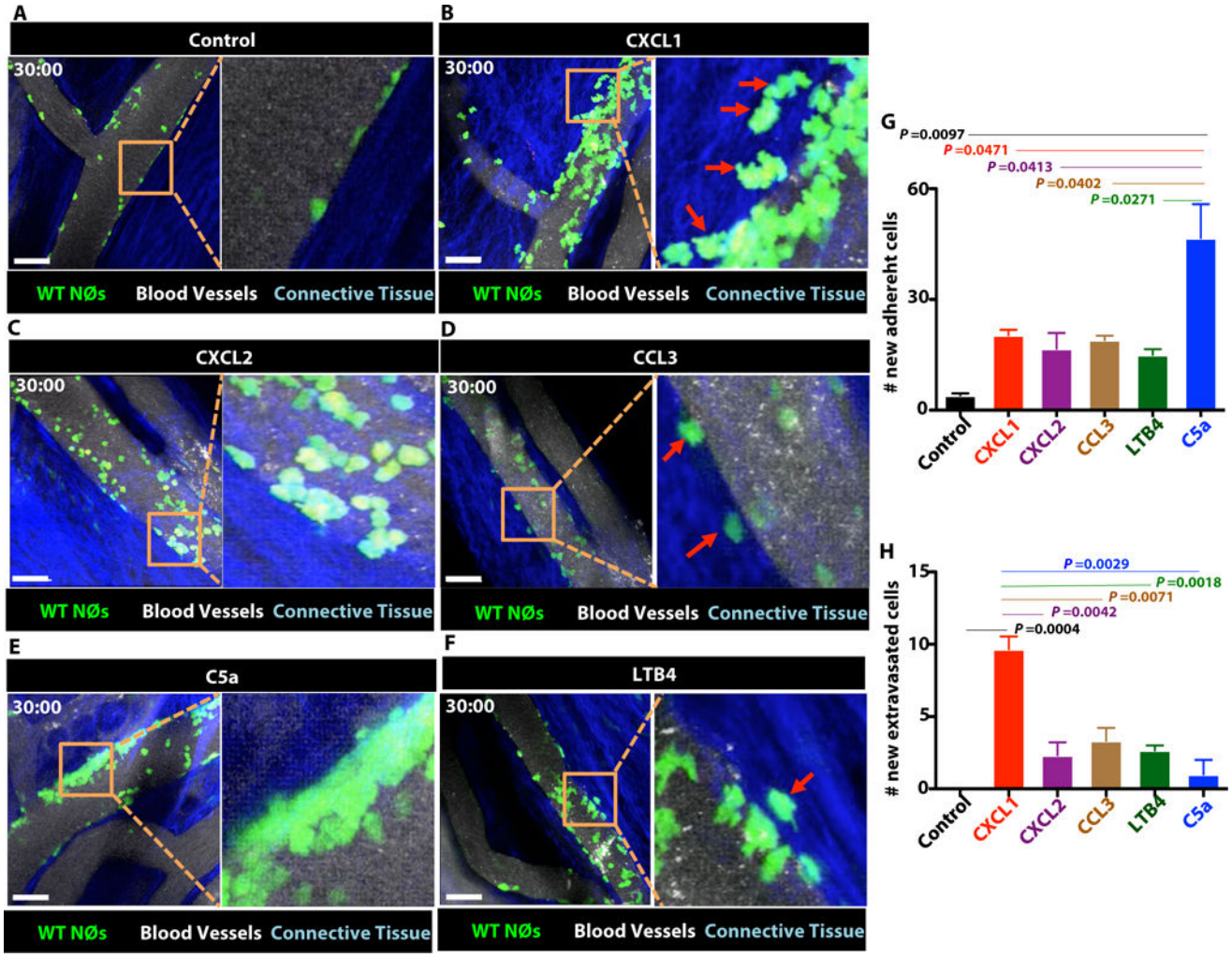

Figure 6. *In vivo* joint adhesion assay

(**A–F**) *In vivo* joint imaging of WT-*LysM*-GFP mice following exposure to CAs (n = 3). (**A**) Control (**B**) CXCL1 (**C**) CXCL2 (**D**) CCL3 (**E**) C5a and (**F**) LTB_4. GFP: neutrophils; Blue: Connective tissue; Qdots: Blood vessels. Time in mins:secs. Scale bars represent 50 μm. Images are representative from 3 independent experiments. (**G**) Number of newly adherent cells and (**H**) newly extravasated in the joints over the 30-min observation after the application of the CA (1nM). (**G, H**) Data indicate mean ± SEM.; n = 3 mice/group; P value calculated using unpaired two-tails Student's t-test.

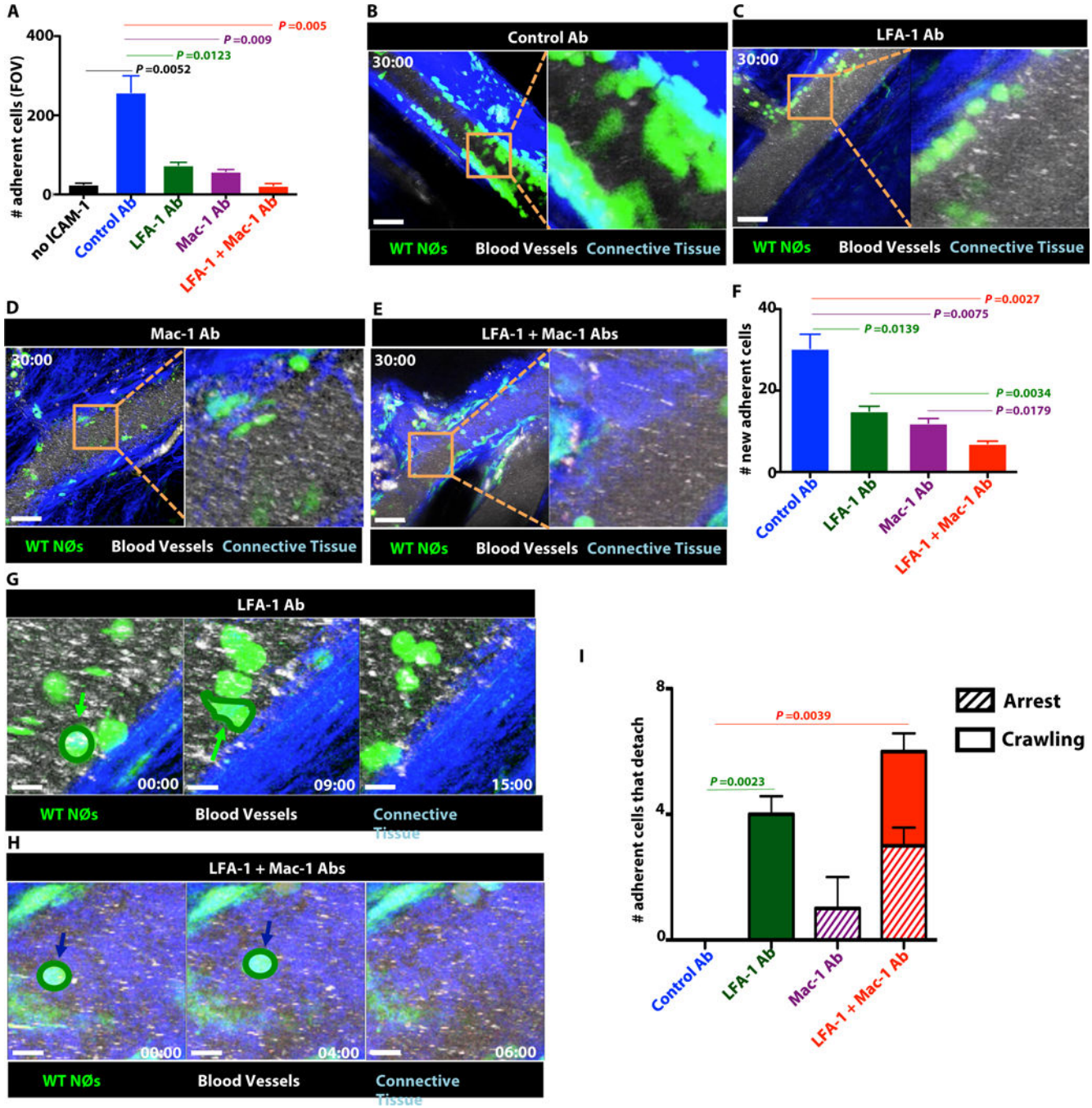

Figure 7. β2 integrin activation mediates C5a-induced neutrophil adhesion to the joint endothelium

(**A**) *In vitro* adhesion of C5a (1 nM) activated WT neutrophils to ICAM-1 coated plates in presence of β2 integrin blocking mAbs or an isotype control mAb. n = 3 independent experiments. Data indicate mean ± SEM; P value calculated using unpaired two-tails Student's t-test. (**B–F**) *In vivo* imaging of joints in WT-*LysM*-GFP mice that were pretreated for 4 hrs with β2 integrin blocking mAbs or an isotype control mAb following exposure to C5a (1nM). (**B**) Control Ab, (**C**) LFA-1 Ab, (**D**) Mac-1 Ab (**E**) LFA-1 and Mac-1 Ab treated

mice. Green: neutrophils; Blue: Connective tissue; Qdots: Blood vessels. Scale bars represent 50 μm. Time in mins:secs. Data are representative of 3 independent experiments. (**F**) Number of newly adherent cells on the joint endothelium over the 30 mins of observation. (**G–I**) Neutrophil detachment *in vivo*. (**G**) LFA-1 Ab, (**H**) Both LFA-1 and Mac-1 Ab treated mice. Green: neutrophils; Blue: Connective tissue; Qdots: Blood vessels. Green arrows indicate crawling cells that detached and blue arrows indicate arrested cells that detach. Time in mins:secs. Scale bars represent 10 μm. Data are representative of 3 independent experiments. (**I**) Number of newly adherent cells that detach over the 30 mins of observation. Striped bar indicates arrested cells that detach and closed bar indicates crawling cells that detach of the total number of adherent cells that detach. (F, I) n = 3 mice/group. Data indicate mean ± SEM; P value calculated using unpaired two-tails Student's t-test.

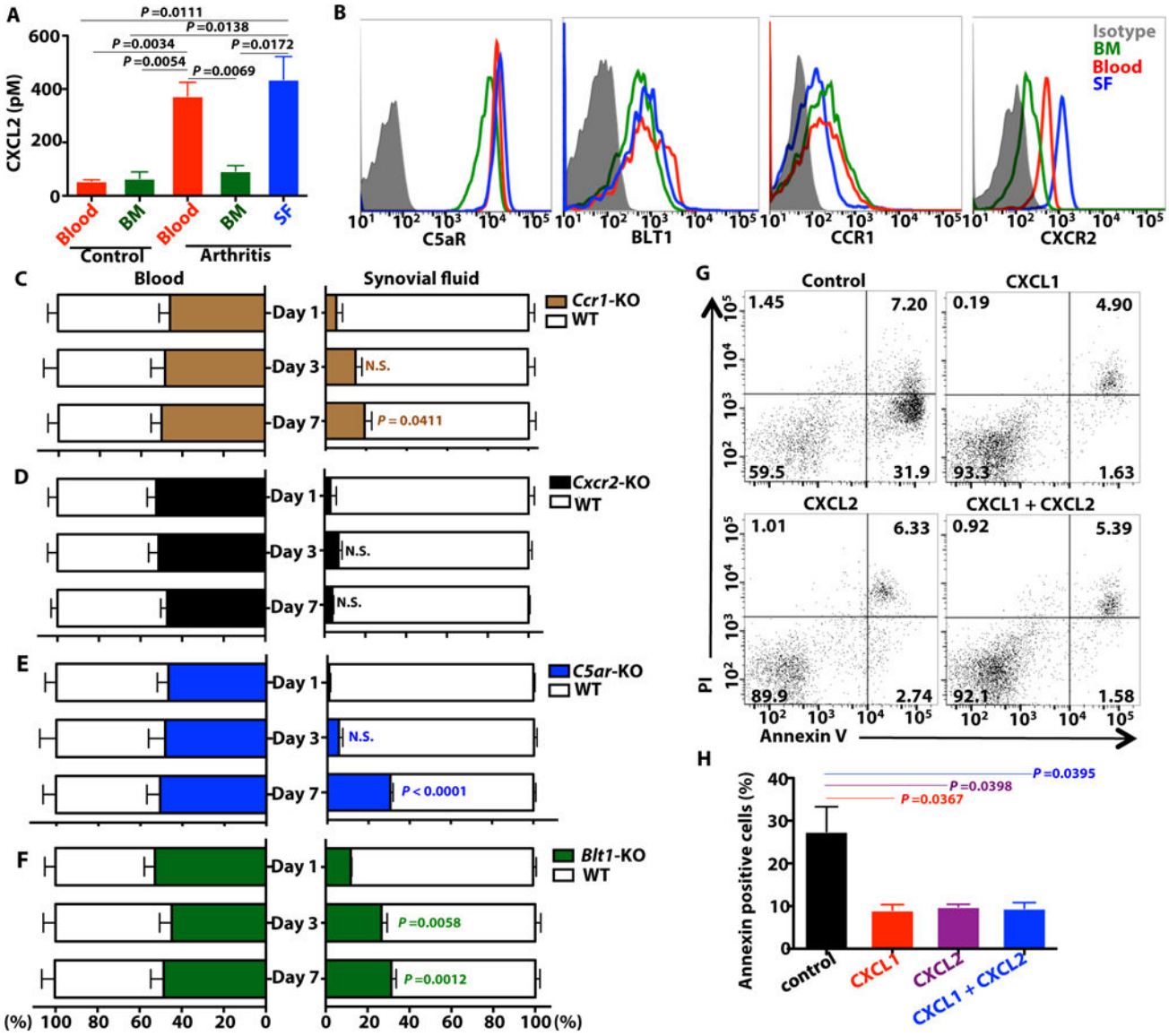

Figure 8. CXCR2 propagates neutrophil recruitment and survival in the joint

(**A**) Quantitation of CXCL2 produced by neutrophils isolated from the BM, blood and SF of WT control and arthritic mice (day 7 following AST). n = 3 mice/group. (**B**) Surface protein CAR expression on neutrophils isolated from the BM, blood and SF of arthritic mice by flow cytometry. Data are representative of 3 independent experiments. (**C–F**) Neutrophils were isolated from blood and SF of mixed BMC mice on day 1, 3 and 7 after AST. WT and (**C**) *Ccr1*-KO, (**D**) *Cxr2*-KO, (**E**) *C5ar*-KO and (**F**) *Blt1*-KO neutrophil in blood and SF were analyzed by flow cytometry. n = 3 independent experiments/time point. (**G, H**) Neutrophils were isolated from SF of WT mice on day 7 after AST and incubated with CXCL1 (1nM) and/or CXCL2 (1nM) for 48 hrs. Neutrophil survival was assessed by flow cytometry using Annexin$^+$ (apoptosis) and PI$^+$ (necrosis) (**G**) and Annexin$^+$ cells quantitated (**H**) n = 3 independent experiments. (**A, C–F, H**) Data indicate mean ± SEM; P value calculated using unpaired two-tails Student's t-test, N.S.- not statistically significant.